Meas. Sci. Technol. **10** (1999) 445–453. Printed in the UK PII: S0957-0233(99)00455-5

On determining *G* using a cryogenic torsion pendulum

R D Newman and M K Bantel

Department of Physics and Astronomy, University of California at Irvine, Irvine, CA 92697-4575, USA

Received 22 December 1998, accepted for publication 15 February 1999

Abstract. A measurement of G which will use a torsion pendulum in the 'dynamic' (time-of-swing) mode, measuring the influence of field source masses on the pendulum's oscillation period, is being prepared at UC Irvine. Features of the design include: (i) operation at cryogenic temperature (2 K) to reduce thermal noise and increase frequency stability and for ease of magnetic shielding, (ii) large pendulum oscillation amplitudes to increase signal-to-noise ratio and reduce the effect of amplitude-determination error, (iii) use of a pair of source mass rings to produce an extremely uniform field gradient; and (iv) use of a thin quartz plate as a torsion pendulum to minimize sensitivity to pendulum density inhomogeneity and dimensional uncertainties. The 'dynamic' method to be used has the great advantage of requiring no angular displacement measurement or calibrating force, but, as pointed out by Kuroda, the method is subject to systematic error associated with the anelastic properties of a torsion fibre. We demonstrate that, for the linear anelasticity discussed by Kuroda, the fractional error introduced by anelasticity in such measurements of G is bounded by $0 \leqslant \delta G/G \leqslant \frac{1}{2}Q^{-1}$, where Q is the torsional oscillation quality factor of the pendulum. We report detailed studies of anelasticity in candidate fibre materials at low temperature, concluding that anelastic behaviour should not limit our G measurement at a level of a few ppm.

Keywords: G, gravitational constant, cryogenic torsion pendulum, torsion balance, torsion pendulum, anelasticity

1. Introduction

Many of the determinations of Newton's gravitational constant G in this century have used a torsion pendulum in a 'dynamic' mode, in which a pendulum suspended by a thin fibre undergoes torsional oscillation in the presence of source masses whose gravitational fields couple to the pendulum's mass multipole moments. Torsional frequencies are compared for two different positions of the source masses. The difference $\Delta\omega^2$ of the squares of the two measured frequencies is proportional to the gravitational constant: $\Delta\omega^2 = cG$, where the proportionality factor c is a known function of the mass distributions and positions of the pendulum and source masses and of the pendulum's oscillation amplitude, but (for an ideal torsion fibre) requires no knowledge of the fibre's torsion constant. The method has several nice features: it is based on a measurement of frequency which can be made with high precision; no precision measurements of angular displacements need be made; and the result is apparently independent of the value of the fibre's torsion constant. However, it has long been suspected that non-ideal fibre properties may lead to unexpected errors in G measurements with this method and Kuroda [1] has shown that anelastic fibre properties do in fact produce such an error through an effective frequency dependence of the torsion constant. Recently reported measurements of G, as well as measurements now in progress or proposed, have mostly either avoided the use of a torsion fibre altogether, or use a fibre in a mode such that it is never subject to significant torsional strain. Other recent approaches use a bifilar suspension [2] or a flat fibre [3] so that the dominant restoring torque on a pendulum is gravitational in origin, thus minimizing possible effects of fibre anelasticity.

The several virtues of the 'dynamic' torsion pendulum method suggest that it may still be the best approach to the measurement of G, even using a single round-section fibre, if anelastic fibre effects are sufficiently well understood and sufficiently small. In the following section we describe the experiment we are developing at UC Irvine for a G measurement using a cryogenic torsion pendulum operating in the dynamic mode, and discuss several novel features of our approach. In subsequent sections we address the issue of anelastic effects. We extend Kuroda's treatment of linear anelastic fibre effects by deriving an upper bound on the effect they can have in a G measurement. We report precision studies of the anelastic properties of candidate fibre materials at low temperature, which reveal a non-linear component of their behaviour which is of considerable intrinsic interest. We reconsider the error bound for G in the light of this

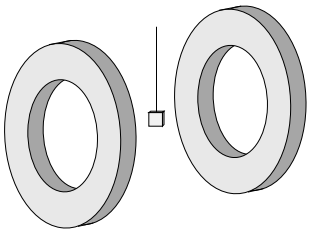

Figure 1. The source-mass and pendulum configuration.

behaviour, and discuss consistency checks that can be made using different fibre materials and oscillation amplitudes to ensure that the *G* measurement can be made reliably at a level of a few parts per million. We also discuss other error sources, including noise in torsional period measurement introduced by the coupling of the pendulum's rocking oscillation modes into the torsional mode.

2. The planned UC Irvine *G* measurement

2.1. The method

The planned experiment determines *G* by measuring the change in oscillation frequency of a thin-plate torsion pendulum when a pair of ring-shaped source masses (figure 1) is moved so that their symmetry axis is alternately parallel and perpendicular to the plane of the pendulum in its equilibrium position.

The source-mass rings produce an extremely uniform gravitational field gradient at the position of the pendulum, making the measurement highly insensitive to error in pendulum position. The use of a thin plate as the pendulum makes the measurement very insensitive to uncertainty in the pendulum's exact dimensions and mass distribution. (Such use of a thin plate and also the use of source masses configured to produce a very uniform field gradient has been independently suggested and implemented by Jens Gundlach see [4]). The pendulum will operate in a cryogenic environment at 2 K, which has several advantages: thermal noise is greatly reduced (directly through the low temperature and indirectly through the higher mechanical Q); the stability of the pendulum's oscillation frequency is greatly increased both by the excellent temperature control possible at low temperature and because the temperature dependences of the pendulum dimensions and fibre shear modulus become small at low temperature; and other fibre properties such as strength and equilibrium-position stability improve at low temperature. An advantage of our design is that the pendulum will operate in a relatively large chamber, minimizing pendulum–wall interactions, and will be far from the source mass, reducing sensitivity to source-mass inhomogeneity and placement error. A price paid for these advantages is a small signal strength: the fractional frequency shift in our experiment will be three orders of magnitude smaller than that in the 1982 experiment of Luther and Towler [5], implying a greater sensitivity to various noise sources, especially microseismic noise.

The experiment will operate in a former Nike missile bunker on an arid-lands environmental preserve at Hanford in Eastern Washington, where the microseismic background

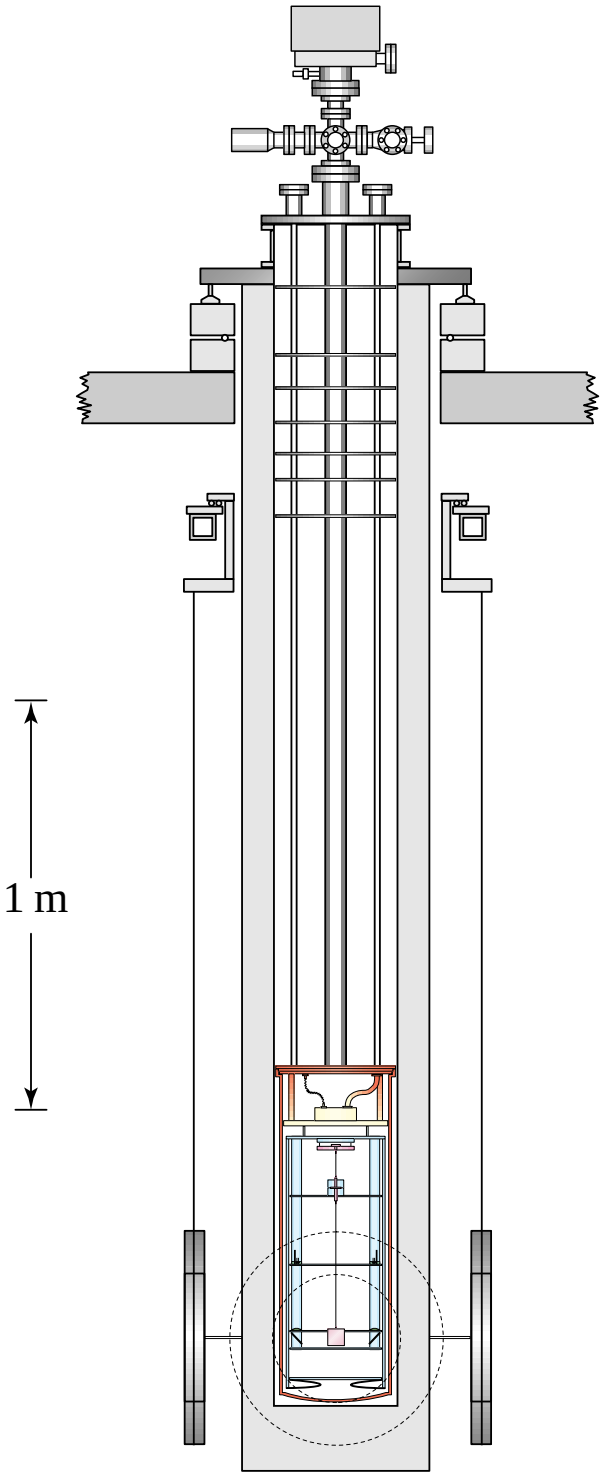

Figure 2. The cryogenic insert within its Dewar flask and source-mass rings suspended from a turntable.

noise is extremely low. The basic instrument being built for the *G* measurement was originally designed to be used for a test of the equivalence of inertial and gravitational mass using a pendulum carrying test masses of two types; it will later serve this purpose as well with minimal modifications.

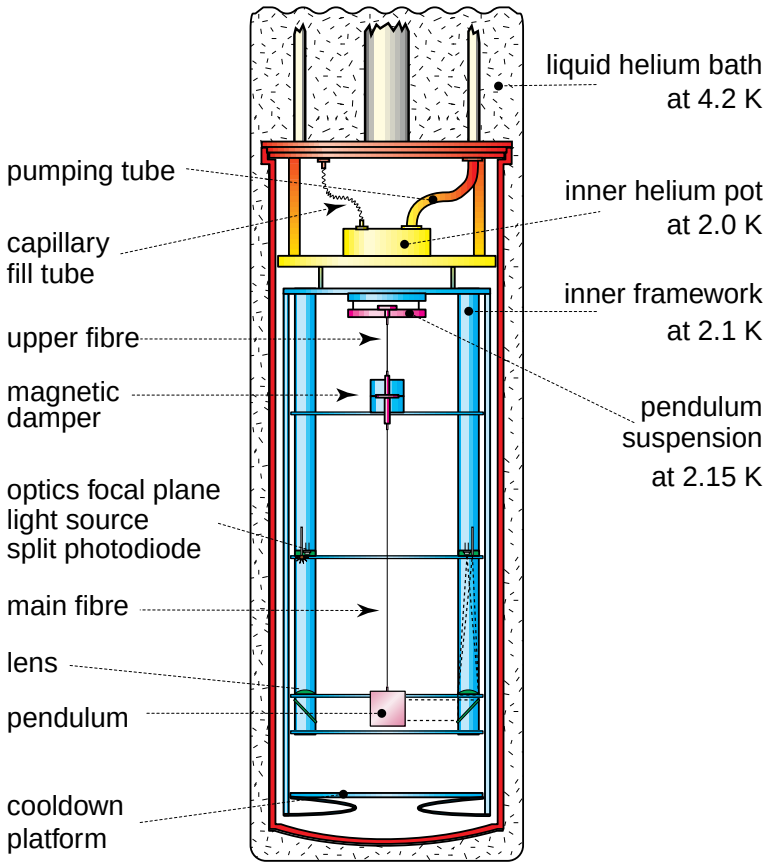

Figure 3. Details of the temperature-controlled levels, pendulum optical readout and damping.

2.1.1. Design details. Figure 2 is a scale drawing showing the size and relative positions of the source-mass rings, the pendulum and the evacuated pendulum housing within the liquid helium Dewar flask.

2.1.1.1. The helium Dewar flask. The Dewar flask is 46 cm in diameter, 290 cm in height and accommodates a 30 cm diameter insert; its helium-holding time is expected to be about 8 days. The Dewar flask is mounted on a turntable which is belt-driven by a stepper motor; by periodically rotating the Dewar flask in alternate directions, the torsional oscillations of the pendulum within it may be resonantly driven to any desired amplitude.

2.1.1.2. The source mass rings. The two source-mass rings will hang outside the Dewar flask at room temperature, suspended by 1.3 mm diameter Kevlar thread from a turntable near the top of the Dewar flask. Three rings have been fabricated for us by the Los Alamos National Laboratory; they are made of OFHC copper, with outside diameter 52.07 cm, inside diameter 31.24 cm, width 4.83 cm and mass 59 kg. To minimize mass changes due to surface oxidation, the rings are plated with an 8 μm non-magnetic coating of nickel with 9% phosphorus. The density of the plating is close to that of the copper, minimizing errors arising from uncertainty in the plating thickness. A dimensionally critical 64.8 cm spacing of the two rings will be maintained by a pair of 8 mm diameter fused silica rods extending between them.

2.1.1.3. The pendulum and torsion fibre. The pendulum is being fabricated of Corning 7980-0AA fused silica, with dimensions 40 mm by 40 mm by 3 mm and mass 10.9 g. The four sides of the pendulum form mirror surfaces, coated with a 100 nm layer of aluminium and a 27 nm layer of SiO_2. An aluminium coating was chosen in preference to gold to minimize uncertainty in mass distribution associated with uncertainty in coating thickness. The pendulum suspension has two stages: an upper relatively thick short fibre which suspends an aluminium damping disc between a pair of ring magnets; and a 30 cm long main torsion wire which extends from this disc down to the pendulum. Eddy-current damping in the disc serves to damp swinging modes of the pendulum without significantly reducing the mechanical Q of the torsional oscillation mode. The main torsion wire will normally be 25 μm diameter Al5056, loaded by the pendulum to about 35% of its breaking strength. With this fibre the pendulum will have a torsion constant of about 0.036 dyn cm rad^{-1} and an oscillation period of 130 s. Data will also be collected using a 20 μm diameter CuBe fibre; comparison of these data with data obtained using an aluminium fibre will provide a test for possible fibre-related systematic error in the determination of G.

2.1.1.4. Temperature control. Figure 3 shows details of the pendulum temperature-control system and optics within the vacuum chamber in which the pendulum operates. Four levels of temperature control are to be maintained. The helium within the main Dewar-flask volume will be pressure controlled to maintain a temperature near 4.2 K. A thermally isolated secondary helium chamber within the vacuum chamber will draw helium through a capillary tube from the main chamber. By pumping on this chamber at a rate governed by a germanium temperature sensor and PID control system, the temperature of a plate coupled to the chamber will be maintained near 2.0 K. An inner framework and enclosure is suspended from this plate with thermally isolating legs; a sensor/heater/PID system will maintain this framework near 2.1 K. Finally, the pendulum is to be suspended from a small platform mounted with thermally isolating legs to the 2.1 K framework. This platform will have its own sensor/heater/PID system which will maintain it at a precisely controlled temperature near 2.15 K. With this multi-level system we expect to maintain temperature control of the torsion fibre to at least within 100 μK, probably much better, even when refilling the main Dewar-flask volume with helium. During installation and initial cooling down, a platform will be raised to support and cool the pendulum. This cooldown platform is linked by flexible copper strips to the 2.1 K enclosure and may be raised by Kevlar threads extending through the main vacuum tube up to a shaft coupled to a rotary vacuum feedthrough at room temperature. We plan to bring the contents of the vacuum chamber to an initial temperature of about 6 K by introducing helium gas; after pumping out this gas the time constants for cooling the instrument components to temperatures below their final operating temperatures should be of the order of a few hours.

2.1.1.5. The optical readout. Four independent optical levers view the pendulum, positioned at 90° intervals about the torsion fibre axis. Two of these are portrayed in figure 3. The four optical systems are identical in their mass distribution, thus increasing the mass symmetry about the pendulum. A 62.5 μm optical fibre delivers the light of an LED at room temperature to the focal plane of each optical lever. Light emitted at this point passes through a lens 16 cm below, is reflected towards the pendulum by a 45° mirror and then reflected by the pendulum—when the pendulum's mirror face is perpendicular to the optical axis—back through the same path to a focus on a two-element PIN split photodiode just beside the end of the optical fibre. For two of the optical levers, the axis of the dividing line between the photodiode elements is aligned perpendicularly to the path traversed by the imaged light spot as the pendulum rotates—the zero crossing of the amplified differential signal from the photodiode elements serves to accurately record the times at which the pendulum has one of a set of discrete angular orientations.

To minimize heating of the pendulum by absorption of light power, the LED light sources will be activated only during the few milliseconds during which they can provide useful information—the required timing and duration of these illumination intervals can be accurately predicted after information from the first few pendulum-oscillation cycles has been analysed by the computer.

2.2. The analysis formalism and key design features

2.2.1. The formalism. The gravitational torque on a torsion pendulum due to a field source-mass distribution may be expressed as

$$N(\theta) = \sum_{lm} \mathrm{i}m q_{lm} a^*_{lm}\, \mathrm{e}^{-\mathrm{i}m\theta} \tag{2.1}$$

where θ is the angular displacement of the pendulum relative to the source-mass distribution and the q_{lm} are the mass multipole moments of the pendulum, given by

$$q_{lm} = \int_p \rho_p(\boldsymbol{r}) r^l Y^*_{lm}(\theta, \phi)\, \mathrm{d}^3\boldsymbol{r} \tag{2.2}$$

where the integral is over the pendulum's density $\rho_p(\boldsymbol{r})$ in a body-fixed coordinate system. The a_{lm} are the field multipole moments of the source mass, given by

$$a_{lm} = -\frac{4\pi G}{2l+1} \int_s \frac{\rho_s(\boldsymbol{r})}{r^{l+1}} Y^*_{lm}(\theta, \phi)\, \mathrm{d}^3\boldsymbol{r} \tag{2.3}$$

where the integral is over the source mass density $\rho_s(\boldsymbol{r})$ in a space-fixed coordinate system with its origin centred on the pendulum. If the pendulum executes torsional oscillation with amplitude θ_0, its natural frequency ω_0 will be shifted by the gravitational torque:

$$\omega^2 = \omega_0^2 - \frac{2}{\theta_0 I} \sum_{lm} m q_{lm} a^*_{lm} J_1(m\theta_0) \tag{2.4}$$

where I is the pendulum's moment of inertia. The special feature of the ring source masses is that they generate a field characterized by a_{lm} which vanish for $\ell = 1, 3, 4, 5$—for odd ℓ by symmetry; for $\ell = 4$ as a result of a particular ring spacing. (For a thin ring of diameter D this spacing is $L = D\cot(\theta)$, where θ is a zero of the Legendre polynomial $P_4(\cos\theta)$.) The resulting field, expressed in a Cartesian coordinate system with its origin centred between the rings and with the ring symmetry axis taken to be the x axis, is a potential $\Phi(x, y, z)$ proportional to $-2x^2 + y^2 + z^2 + \mathrm{O}(x^6, y^6, z^6)$. Thus the rings' field couples almost purely to the pendulum's quadrupole moment.

Letting ω_+ and ω_- represent the pendulum's oscillation frequencies corresponding to the two orientations of the ring source masses, one finds that the pendulum's frequency shift associated with the change in ring source-mass positions is given to within a few ppm by

$$\Delta\omega^2 \equiv \omega_+^2 - \omega_-^2 \approx 16|a_{22}|\frac{|q_{22}|}{I}\frac{J_1(2\theta_0)}{\theta_0} \tag{2.5}$$

which we may write in the form

$$\Delta\omega^2 \approx K_{source}\frac{J_1(2\theta_0)}{\theta_0}\left(\frac{Q_2}{I}\right)G \tag{2.6}$$

where G is the gravitational constant to be determined, $Q_2 = (32\pi/15)^{1/2} q_{22}$ and K_{source} is a factor depending *only* on the source-mass distribution relative to the pendulum. Written in this form, we see that $\Delta\omega^2$ depends on the

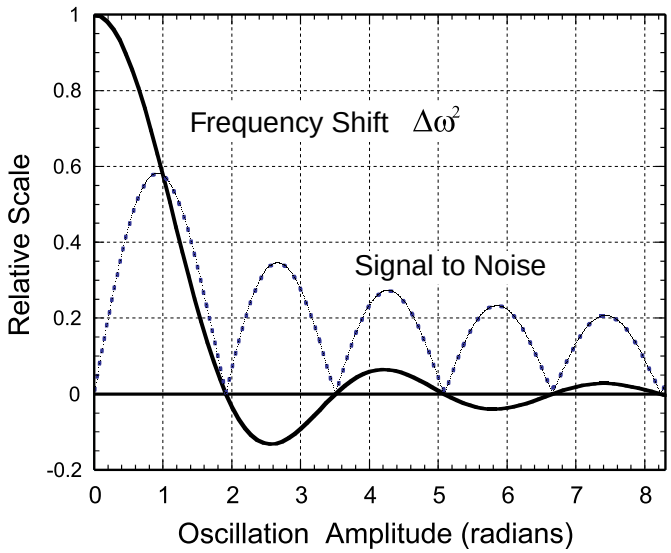

Figure 4. The relative signal strength $\Delta\omega^2/\omega^2$ and signal-to-noise ratio as functions of the oscillation amplitude. Oscillation amplitudes near the extrema of the signal-strength curve will be used in measuring G.

properties of the pendulum only through the ratio of its quadrupole moment Q_2 to its moment of inertia I, with

$$I = \int \rho(\boldsymbol{r})(x^2 + y^2)\,\mathrm{d}^3\boldsymbol{r} \tag{2.7}$$

$$Q_2 = \int \rho(\boldsymbol{r})(x^2 - y^2)\,\mathrm{d}^3\boldsymbol{r} \tag{2.8}$$

where the y axis in the integrals is the direction in which the pendulum is thin.

2.2.2. The advantages of ring source masses and a thin pendulum. We now see the benefits of the rings and a thin pendulum. (i) On comparing equations (2.7) and (2.8) we see that the ratio Q_2/I in equation (2.6) (and hence the measured value of G) depends only very weakly on the pendulum's size and mass distribution if the pendulum is thin. That the dependence of equation (2.6) on pendulum mass distribution is almost purely through the ratio Q_2/I is a consequence of the absence of $\ell = 3$, 4 and 5 couplings of the source-mass rings. (ii) The factor K_{source} in equation (2.6) proves to be extremely insensitive to displacement of the pendulum relative to the source masses—again a consequence of the absence of $\ell = 3$, 4 and 5 couplings. In our design the pendulum may be misplaced by as much as 5 mm horizontally or 10 mm vertically without creating more than a 1 ppm error in the G measurement.

2.2.3. Higher order effects on $\Delta\omega^2$. Corrections must be made to equation (2.6) due to contributions to $\Delta\omega^2$ from terms with $\ell = 6$ and $m = 2$ and 6 in equation (2.4). These calculable corrections are a few ppm.

2.2.4. Large-amplitude operation. Figure 4 displays the relative frequency shift produced by the source rings as a function of the pendulum's torsional oscillation amplitude θ_0. The pendulum will operate at the several large amplitudes (2.57, 4.21, 5.81 and 7.40 radians) at which $\Delta\omega^2$ is an extremum and hence very insensitive to uncertainty in θ_0. (Optical lever timing signals from the four mirrored side faces of the pendulum can determine θ_0 to within microradian accuracy in a single cycle.) Because of the decay in amplitude with time due to the finite Q of the pendulum, it will be necessary to begin a run with an amplitude which is about 50 mrad larger than one corresponding to an extremum and to limit the run duration so that the amplitude remains close enough to the extremum value to afford sufficient insensitivity to amplitude-measurement error. For an Al5056 fibre, the allowed continuous run time ranges from 6 days, for oscillation within 50 mrad of the 2.57 amplitude, to 2 days near the 7.40 amplitude. The change in oscillation period when the source rings are moved will range from 1.6 ms at the 2.57 amplitude to 0.33 ms at the 7.40 amplitude. Noise contributions to frequency measurement decrease with amplitude as $1/\theta_0$, so that the signal-to-noise ratio drops more slowly than does the signal at the larger amplitudes. Comparison of G determinations performed at various oscillation amplitudes will provide an important check for effects of fibre nonlinearities and background torques, which vary with amplitude.

2.3. Metrology issues and noise sources

2.3.1. Metrology. The most critical measurements are of the mass and dimensions of the source rings and of the length of the fused silica rods which maintain the ring spacing. Our goal is to keep the contribution to the total G error budget of each individual metrology component below 1 ppm, which requires that the ring ID, OD and width must each be known to 1 μm and the rod length to 0.5 μm. The spacing of the rings' suspension points is relatively non-critical. The rings have an awkward mass and shape for precision measurement; initial mass measurement at the NIST will probably not be better than 2 ppm inaccuracy. Density measurements of copper stock from which the rings were cut indicate that the density variation over each ring's volume is no more

than about 30 ppm, while the critical average variation over the ring's radius is of the order of 5 ppm, which would produce an error in G of less than 1 ppm if it were ignored. The thermal expansion of the copper rings poses a serious problem, because the temperature in the missile bunker where the experiment is to be run varies seasonally by as much as 10 K. A 30 mK error in the temperature of the rings relative to the temperature at which they were measured will cause a 1 ppm error in G. The rings' temperature will be monitored by platinum resistance thermometers embedded in them.

2.3.2. Thermal kT noise. This contributes an uncertainty in the measured period of a torsion pendulum:

$$\delta\tau \approx \frac{\tau}{\theta_0}\left(\frac{k_B T}{k\omega_0 \mathrm{Q}}\right)^{1/2} t^{-1/2} \tag{2.9}$$

where τ, ω_0, k, Q and θ_0 are respectively the period, angular frequency, torsion constant, quality factor and oscillation amplitude of the pendulum and t is the duration of the measurement. Evaluated for the parameters of our pendulum and $\theta_0 = 2.57$, this implies a 0.04 ppm δG contribution for a measurement duration of 1 week.

2.3.3. Temperature variation. Variation in the temperature of the pendulum's fibre will change its torsion constant, introducing a noise source in frequency measurements. Fortunately the fractional variation of the shear modulus with temperature for Al5056 at low temperature is extremely small, of the order of 2×10^{-7} K^{-1} [6]. For a G error contribution <1 ppm in 1 week we need only ensure that the noise spectrum for temperature variation is less than about 0.3 K Hz$^{-1/2}$ at the signal frequency of about 1 mHz, which should not be difficult.

2.3.4. Sensor shot noise. The light intensity to be used in the optical lever is a compromise between a low photon shot noise (favouring a high intensity) and a small temperature rise of the pendulum from absorption of light power (favouring a low intensity). We calculate that a light intensity low enough to raise the pendulum's temperature by less than 1 mK should introduce a shot-noise contribution to G error of about 0.5 ppm for 1 week of measurement.

2.3.5. Gravitational noise Noise from changing ambient mass distributions is difficult to estimate, but should be extremely small at our signal frequency at our remote site, except possibly during the winter rainy season.

2.3.6. Rotational microseismic noise. This introduces a period timing error given by

$$\delta\tau = \frac{\tau}{2\theta_0}[\theta^2(\omega_0)]^{1/2} t^{-1/2} \tag{2.10}$$

where $\theta^2(\omega_0)$ is the noise spectrum for rotational ground motion, τ, ω_0 and θ_0 are respectively the pendulum's period, angular frequency and amplitude and t is the measurement duration. A few data on rotational seismic noise exist [7], which are approximately fitted by $\theta^2(f) = 10^{-23} f^{-2}$ in the frequency range 0–20 mHz. Assuming this function, the contribution to our G error for 1 week of measurement would be 0.04 ppm.

2.3.7. Linear microseismic noise—the coupling of swinging modes to torque. The coupling of swinging modes into the torsional mode of a pendulum is a source of noise which has been analysed by Speake and Gillies [8] and extensively by Karagioz *et al* [9]. One finds that a pendulum which is rotating with instantaneous angular velocity $\dot{\theta}$ about a horizontal axis experiences an angular acceleration about the vertical fibre axis given by

$$\ddot{\Psi} = \frac{I_2 - I_1}{2I_3}\sin(2\Psi)\dot{\theta}^2 \tag{2.11}$$

where I_1, I_2 and I_3 are the moments of inertia of the pendulum about its body-fixed principal axes and Ψ is the angle between the horizontal rotation axis and principal axis number 1. To estimate how much our G measurement may be affected by torsion noise coupled by this mechanism, we performed a computer simulation, modelling our compound pendulum which has three elements: an upper fibre extending from a lab-fixed pivot down to a mass at which horizontal damping is applied, with a torsion fibre extending from this damping point down to a square thin pendulum body. The equations of motion were determined for the system's seven degrees of freedom: three angles in each vertical plane, plus a rotational degree of freedom about the vertical axis for the pendulum body, using small-angle approximations for all but the vertical axis rotation. In the simulation, the pendulum was 'set in torsional oscillation' with an amplitude corresponding to that in our planned G measurement, while a horizontal acceleration noise spectrum was simulated for the upper suspension point in both horizontal directions, with the spectral shape matching that observed at our experiment site. The equations of motion for the system with this driving force were integrated through multiple cycles of the torsional oscillation, while noting the RMS variation $\delta\tau$ (RMS) in torsional period determined by the apparent zero crossings of the torsional variable Ψ. The resulting value of $\delta\tau$ (RMS) proved to be proportional to the square of the driving noise spectrum, as would be expected from equation (2.11). The simulation was repeated for various degrees of the damping; for optimal damping the results when extrapolated to the very low seismic noise amplitudes measured at our Hanford site indicate that the contribution to G error of noise through this coupling mechanism should be negligible—about 0.001 ppm for 1 week of measurement.

2.3.8. Other vibration issues. Vertical microseismic motion can couple into torsional noise through nonlinearities in the fibre's response to vertical spring-type oscillation modes of the pendulum—we have no estimate of this error. We also do not know how much vibration noise will be contributed by the evaporating helium, although we do know that this is small compared with other sources of vibration noise at our lab in Irvine. It should also be noted that there may be 'snap-crackle–pop' noise originating in our fibre and/or mounts which is not accounted for in the preceding paragraphs.

2.3.9. Empirical noise estimation. We have used data taken with an azimuthally symmetrical pendulum in our

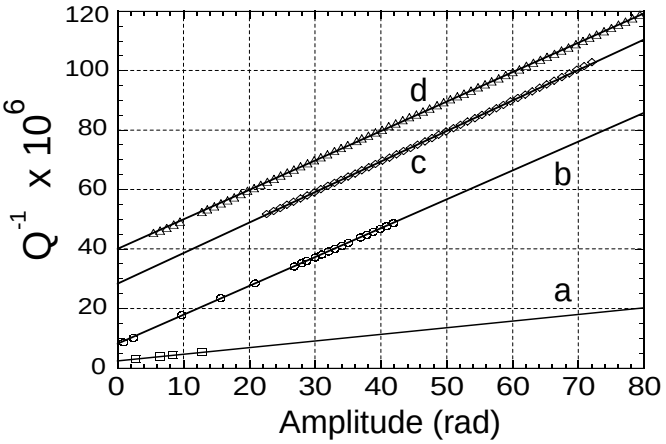

Figure 5. Q^{-1} versus the oscillation amplitude for (*a*) a 50 μm Al5056 fibre at 4.2 K and a 20 μm CuBe fibre at (*b*) 4.2 K, (*c*) 77 K and (*d*) 77 K with epoxy drops on the fibre. Lines are linear fits. The pendulums with Al5056 and CuBe fibres oscillated at 10 and 6 mHz respectively.

lab at Irvine to put an upper limit on the total noise to be expected from all sources except for gravitational sources and swing–torque coupling effects. Data from a 10 h run in 1996 were treated as a fake G measurement, in which source rings were imagined to have been moved. The (zero) 'period difference signal' in this mock experiment was measured to within an accuracy of 130 ns; this noise level would permit a G measurement to about 40 ppm in a period of 1 week. Seismic noise will be nearly two orders of magnitude smaller at our Hanford site and our temperature control will be vastly better with the new apparatus. Hence we are optimistic that noise levels at the Hanford site will not contribute more than a few ppm to uncertainty in a G measurement lasting 1 week.

3. Effects of fibre nonlinearity and anelasticity

3.1. A bound on G measurement error from linear fibre anelasticity

Kuroda [1] has shown that, in a G measurement using the dynamic method, the frequency dependence of the effective fibre torsion constant can introduce a systematic error. Kuroda evaluated this error for the case discussed by Quinn *et al* [10] of an anelastic material characterized by a continuum Maxwell model [11] with a particular assumed distribution of relaxation strengths. Kuroda also showed that, if the imaginary part of the torsion constant is a fixed fraction ϕ of the real part, then the fractional bias in G will be equal to Q^{-1}/π, where Q is the pendulum's quality factor. Here we show that, if the fibre anelasticity is described by a continuum Maxwell model with *any* distribution of relaxation strengths, the resulting error $\delta G/G$ will be bounded between 0 and $\frac{1}{2}Q^{-1}(+\mathrm{O}(Q^{-2}))$.

Let the complex torsion constant be expressed as $k(\omega) = k_0 + k_1(\omega) + \mathrm{i}k_2(\omega)$, where k_0, the 'relaxed' (zero frequency) limit of k, is the dominant term. In the dynamic method of G measurement, the presence of the source masses effectively changes k_0. The resulting effective change in k, which determines the oscillation frequency, includes an indirect contribution from $k_1(\omega)$ due to the frequency shift. If this contribution is neglected the resulting error in G determination is

$$\frac{\delta G}{G} = \left(\frac{\partial \operatorname{Re} k}{\partial k_0} - 1\right) = \frac{\partial k_1}{\partial \omega^2}\frac{\partial \omega^2}{\partial k_0} \approx \frac{\partial k_1}{\partial \omega^2}\frac{\omega^2}{k_0}. \tag{3.1}$$

In the continuum Maxwell model, k_1 and k_2 are expressed in terms of a distribution of relaxation strengths $F(\tau)$ ($F(\tau) = \delta E f(\tau)$ in the notation of Quinn *et al* [10]):

$$k_1(\omega) = \int_0^\infty F(\tau)\frac{\omega^2\tau^2}{1+\omega^2\tau^2}\,\mathrm{d}\tau \tag{3.2}$$

$$k_2(\omega) = \int_0^\infty F(\tau)\frac{\omega\tau}{1+\omega^2\tau^2}\,\mathrm{d}\tau. \tag{3.3}$$

From equations (3.1) and (3.2) we find

$$\frac{\delta G}{G} = \frac{1}{k_0}\int_0^\infty F(\tau)\frac{\omega^2\tau^2}{(1+\omega^2\tau^2)^2\,\mathrm{d}\tau}. \tag{3.4}$$

The Q of the pendulum is given approximately by k_0/k_2, so

$$\frac{1}{Q} = \frac{1}{k_0}\int_0^\infty F(\tau)\frac{\omega\tau}{1+\omega^2\tau^2}\,\mathrm{d}\tau. \tag{3.5}$$

Here ω is the pendulum's oscillation frequency. Equation (3.4) differs from (3.5) only by an extra factor $\omega\tau/(1+\omega^2\tau^2)$ in the integrand which has a value $\leqslant\frac{1}{2}$ for all values of τ. Because the other factors in the integrands are all positive, we find the following bound on G error in the general model discussed by Kuroda: $0 \leqslant \delta G/G \leqslant \frac{1}{2}Q^{-1} + \mathrm{O}(Q^{-2})$, where the higher order term $\mathrm{O}(Q^{-2})$ reflects the approximation made in equation (3.1).

3.2. Measurements of fibre properties at low temperature

For the past several years we have been measuring the Q's of symmetrical torsion pendulums using various fibre materials (tungsten, sapphire, CuBe and Al5056) at low temperature, in search of materials offering the highest Q. Al5056 appears to be the best choice, yielding a Q at 4.2 K which is over 300 000. The $\frac{1}{2}Q^{-1}$ bound on G error then suggests that

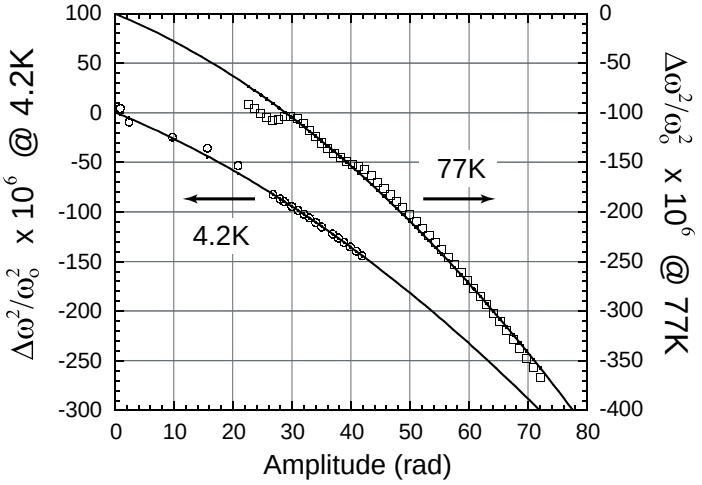

Figure 6. $\Delta\omega^2/\omega^2$ versus amplitude for a CuBe fibre, compared with expectation (solid lines) for a stick–slip mechanism (equation (3.7)).

the systematic bias due to anelasticity in our planned G measurement should be less than 2 ppm.

However, Kuroda's analysis and our extension of it assume linear anelasticity. In that framework the effective torsion constant will depend on frequency but cannot depend on oscillation amplitude. But, in fact we find a significant dependence of Q on amplitude: for an Al5056 fibre, Q varies by about 20% between zero amplitude and the range of shear-stress amplitudes involved in the projected G measurement. To study such behaviour we have concentrated our attention on a CuBe fibre, for which the amplitude dependence is ten times larger.

Figure 5 displays measured values of Q^{-1} for azimuthally symmetric pendulums using fibres of Al5056 and CuBe, as a function of the oscillation amplitude. Note that, for the CuBe fibre, Q^{-1} is an extremely linear function of amplitude, with a slope which is nearly the same at 4.2 and 77 K but with a zero-amplitude intercept differing by a factor of 3.5 at these two temperatures. The amplitude dependence is not associated with the Stycast 1266 epoxy fibre mount: amplifying the epoxy-related loss by a factor of five by placing four drops of epoxy along the fibre changes the zero amplitude limit of the Q^{-1} plot significantly but not its slope (figure 5(*d*)).

These data suggest that the CuBe fibre's internal friction has two independent contributions: $Q^{-1} = Q_I^{-1}(T) + Q_{II}^{-1}(A)$, where Q_I^{-1} is temperature dependent but amplitude independent, while Q_{II}^{-1} is amplitude dependent but not temperature dependent. The temperature independence of Q_{II}^{-1} suggests that no time-dependent relaxation is involved in its underlying mechanism and therefore that the mechanism should be frequency independent and thus not a source of bias in the G measurement. A linear dependence of Q^{-1} on amplitude is characteristic of a 'stick-slip' model of hysteretic loss—a model which is in fact frequency independent. This model also predicts a dependence of the oscillation frequency ω^2 on amplitude A, related to the amplitude-dependent part of Q^{-1} by

$$\Delta\omega^2/\omega^2 = -(3\pi/4)\Delta Q^{-1}$$

where

$$\Delta\omega^2 = \omega^2(A) - \omega^2(0)$$

and

$$\Delta Q^{-1} = Q^{-1}(A) - Q^{-1}(0).$$

This relation is closely satisfied by our data if we include a contribution to $\Delta\omega^2$ which must arise from an elastic coefficient k_3 in the conservative part of the torsion constant: $\tau = -(k\theta + \cdots + k_3\theta^3 + \cdots)$. We determine k_3 very precisely from our data by measuring the harmonic it produces in the pendulum's torsional oscillation:

$$\theta(t) = A\sin(\omega t) + \cdots + \frac{-A^3}{32}\frac{k_3}{k}\sin(3\omega t) + \cdots. \qquad (3.6)$$

Including the contribution of k_3 to ω^2 and assuming a stick–slip contribution, we then expect

$$\frac{\Delta\omega^2(A)}{\omega^2} = -\frac{3\pi}{4}\Delta Q^{-1}(A) + \frac{3}{4}\frac{k_3}{k}A^2. \qquad (3.7)$$

Figure 6 compares our measured $\Delta\omega^2(A)$ with this relation. The coefficient of $\Delta Q^{-1}(A)$ inferred by fitting our data equals the factor $3\pi/4$ expected from stick–slip to within 25% at 77 K and to within better than 1% at 4.2 K.

3.3. Implications for a G measurement

We have demonstrated that linear anelasticity need not limit a G measurement at a level down to about 2 ppm or less. (We note, however that the result of a recent experiment by Kuroda *et al* [12] suggests that the frequency dependence of a fibre's torsion constant may exceed the limit we have derived in section 3.1.) Our measurements give strong evidence that the amplitude-dependent component of the damping we observe arises from a stick–slip mechanism which, being frequency-independent, will have negligible influence on the G measurement. In any case, the amplitude-dependent component of Q^{-1} is only a small fraction of the total damping in our planned experiment: at an oscillation amplitude of 2.57 radians it contributes 25% of the damping using a CuBe fibre, and less than 10% of the (smaller) damping using an Al5056 fibre. Let us suppose that the amplitude-dependent component is *not* frequency-independent, but in fact contributes a fractional G error given

by Q_{II}^{-1}/π like that expected for linear anelasticity. Then, for the aluminium fibre this error contribution would range from 0.08 ppm at oscillation amplitude 2.57 radians to 0.22 ppm at 7.40 radians, whereas the contributions for the CuBe fibre would range from 0.8 ppm to 2.3 ppm. Correspondingly, the *total* G error introduced by anelasticity for these amplitudes would (if it were ignored) range from 1.0 to 1.2 ppm for the Al5056 fibre, and from 3.5 to 5.0 ppm for the CuBe fibre.

Attention must also be paid to effects of elastic fibre non-linearity and to torques on the pendulum arising from lab-fixed electromagnetic or gravitational fields. These generate a torque on the pendulum of the form:

$$N(\theta) = -(k_1\theta + k_2\theta^2 + k_3\theta^3) + \sum [a_n \cos(n\theta) + b_n \sin(n\theta)].$$

To first order these torque terms contribute nothing to the change in pendulum-oscillation frequency when the source masses are moved. Numerical integrations of the equations of motion demonstrate that, at higher order, these terms affect a G measurement by less than 1 ppm. Since the coefficients in this equation may be experimentally measured with high precision, these effects pose no problem for a G measurement.

We conclude that fibre-related problems need not introduce more than a 3 ppm uncertainty into a G measurement with our apparatus. Ultimately the absence of significant fibre-related error in our measurement of G must be demonstrated by the consistency of measurements made at various amplitudes with fibres of varying properties.

Acknowledgments

We thank Arthur Nowick and T J Quinn for many discussions of anelasticity and fibre behaviour. We are greatly indebted to Haskell Sheinberg, Paul Dunn and Bill Baker of the Los Alamos National Laboratory for the fabrication of precision source-mass rings; to Lee Moritz, Richard Busby and Ron Hulme of the UCI machine shop for fabrication of many experiment components; and to our undergraduate assistants Hugo Rico, Gilberto Rodriguez, David Schorr and David Fiske.

We are particularly indebted to Roy Gephart and the Battelle Pacific Northwest Laboratory for all they have done to make a remote lab available; and to Paul Boynton for sharing it with us. Our work is funded by NSF grant PHY-9514944.

References

[1] Kuroda K 1995 *Phys. Rev. Lett.* **75** 2796
[2] Luther G private communication
[3] Quinn T J, Speake C C and Davis R S 1997 *Metrologia* **34** 245
[4] Gundlach J H, Adelberger E G, Heckel B R and Swanson H E 1996 *Phys. Rev.* D **54** R1256
[5] Luther G G and Towler W R 1982 *Phys. Rev. Lett.* **48** 121
[6] Adams P W and Jing-Chun Xu 1991 *Rev. Sci. Instrum.* **62** 2461
[7] Stedman G E, University of Canterbury, Christchurch New Zealand (private communication to Paul Boynton, University of Washington)
[8] Speake C C and Gillies G T 1987 *Z. Naturf.* a **42** 664
[9] Agafanov N I, Voronkov V V, Izmaylov V P and Karagioz O V 1975 *Phys. Solid Earth* **11** 69
[10] Quinn T J, Speake C C and Brown L M 1992 *Phil. Mag.* A **65** 261
[11] Nowick A S and Berry B S 1972 *Anelastic Relaxation in Crystalline Solids* (New York: Academic) ch 4
[12] Matsumura S, Kanda N, Tomaru T, Ishizuka H and Kuroda K 1998 *Phys. Lett.* A **244** 4